Transformations for Evaluating Singular Boundary Element Integrals *

Peter R. Johnston

School of Science

Griffith University

Kessels Road

Nathan

Queensland 4111

Australia

David Elliott

Department of Mathematics

University of Tasmania

GPO Box 252-37

Hobart

Tasmania 7001

Australia

January 14, 2002

*This work was supported by the Australian Research Council.

Abstract

Accurate numerical integration of line integrals is of fundamental importance for the reliable implementation of the boundary element method. Usually, the regular integrals arising from a boundary element method implementation are evaluated using standard Gaussian quadrature. However, the singular integrals which arise are often evaluated in another way, sometimes using a different integration method with different nodes and weights.

This paper presents a straightforward transformation to improve the accuracy of evaluating singular integrals. The transformation is, in a sense, a generalisation of the popular method of Telles with the underlying idea being to utilise the same Gaussian quadrature points as used for evaluating non–singular integrals in a typical boundary element method implementation. The new transformation is also shown to be equivalent to other existing transformations in certain situations.

Comparison of the new method with existing coordinate transformation techniques shows that a more accurate evaluation of weakly singular integrals can be obtained. The technique can also be extended to evaluate certain Hadamard finite–part integrals. Based on the observation of several integrals considered, guidelines are suggested for the best transformation order to use (ie the degree to which nodes should be clustered near the singular point).

Key words: nonlinear coordinate transformation, boundary element method, weakly singular integrals, numerical integration, Hadamard finite–part integrals.

1 Introduction

Weakly singular line integrals arise in the boundary element method when the source point lies on the element over which the integration is to be performed. When considering, for example, the two dimensional Laplace equation, the boundary element kernel is of the form $\ln \frac{1}{r}$ where r is the distance from the source point to the integration point. Hence, multiplication of this kernel by some basis function, ϕ, and subsequent integration over the current element, Γ, gives rise to a weakly singular integral of the form

$$g = \int_{\Gamma} \ln \frac{1}{r} \phi d\Gamma. \tag{1.1}$$

There are several methods available to evaluate the above integral, most of which fall into the categories of either coordinate transformation (to increase the smoothness of the integrand at the singular point) [1, 2, 3, 4] or interval splitting [5, 6, 7, 8]. The idea behind both categories of techniques is to use the same Gaussian quadrature points and weights as those used for the non–singular integrals. For example, if 10 Gaussian points and weights are used to evaluate the non-singular integrals, it is desirable to use the same 10 points and weights to evaluate the singular integrals. The first category of techniques, coordinate transformation, would simply relocate these 10 points on the interval of integration to improve the accuracy of the evaluation of the singular integral. On the other hand, the second category of techniques, interval splitting, splits the interval at the singularity and uses the 10 points on each subinterval, requiring a total of 20 evaluations of the integrand, instead of 10. An ideal interval splitting method should more accurately evaluate a singular integral using the same 10 Gaussian points twice, than a coordinate transformation technique using 20 Gaussian points over the entire interval. As a result, this will reduce storage requirements and operation counts in the computer code implementing the numerical methods, as only the nodes and weights for the 10 point Gaussian quadrature rule need to be determined and stored. Other possible techniques for

evaluating these integrals include using a completely different set of integration points and weights dependent on the kernel [9] and integral simplification [1, 10]. We shall say no more of these methods.

It has recently been shown [11] that a nonlinear transformation, introduced by Monegato and Sloan [12] and subsequently used by Scuderi [13] to study flow around an airfoil with flap, can be used to evaluate integrals of the form (1.1). This is a polynomial transformation of arbitrary odd degree, with zero Jacobian at the singularity which does not require the interval of integration to be split at the singularity. Hence it falls into the first of the two categories, i.e. coordinate transformation, for numerical evaluation of singular integrals described above.

The transformation of Monegato and Sloan works well when the singularity is at the end points of the interval. On the other hand, as it may be seen from Tables 4, 5 and 6, relative errors can be reasonably large at other points of the interval for lower order transformations. Of course, the method can be improved by first splitting the interval of integration at the singularity and applying the Monegato–Sloan transformation on each subinterval. In this case, the transformation no longer has to be of odd degree and the transformation due to Sato *et al.* [5] is recovered. The popular transform due to Telles [2] arises as a special case of the Monegato–Sloan transformation when the polynomial is of degree three.

The method outlined below is an interval splitting technique which arose from a recent study of semi–sigmoidal transformations [7] and their subsequent numerical analysis [8]. It turns out that this technique is related to the techniques of Telles and Monegato and Sloan when the singularity is at one of the end points of the interval.

The next section of the paper describes the integrals of primary interest in this paper and the following section introduces the coordinate transformation to be studied. In section four several integrals, which compare the relative accuracy of this method with existing techniques, are evaluated and in section five the technique is generalised to consider certain Hadamard

finite–part integrals.

2 Weakly Singular Integrals

This paper is primarily concerned with evaluation of boundary element method line integrals of the form given in equation (1.1) where, as mentioned previously, Γ is an arbitrary boundary element in two dimensional space, r is the distance from the source point (x_0, y_0) to the element Γ and ϕ is a basis function. The usual practice is to transform the integral into one along the path from -1 to 1 in a local coordinate system, resulting in the integral

$$g = \int_{-1}^{1} \ln \frac{1}{r(s)} \phi(s) J(s) ds, \tag{2.1}$$

where $J(s)$ is the Jacobian of the transformation. Assuming that the singularity occurs at some point s_0, $-1 \leq s_0 \leq 1$, in the local coordinate system, then $r(s) = |s - s_0|$.

Although the integrals of concern to boundary element method practitioners usually contain a weak singularity of the logarithmic type, the methods to be described here apply equally well to weakly singular integrals having an algebraic singularity at s_0,

$$g_\alpha = \int_{-1}^{1} |s - s_0|^\alpha \phi(s) J(s) ds \tag{2.2}$$

where $\alpha > -1$.

We aim to evaluate the integral in equation (2.1) using Gauss-Legendre quadrature with the same integration weights and node points as for the non–singular integrals arising in a boundary element method formulation. The next section describes what is effectively a transformation of these points and weights which results in an accurate evaluation of weakly singular integrals.

3 A Monomial Transformation

The motivation for this approach began with recent work on sigmoidal and semi–sigmoidal transformations (see [14] and [7], respectively). In general a sigmoidal transformation, γ_r, of the interval [0,1] onto itself is a function of the form (see [14])

$$\gamma_r(t) := \frac{f_r(t)}{f_r(t) + f_r(1-t)}, \quad 0 \leq t \leq 1, \tag{3.1}$$

where $f_r(t) = O(t^r)$ near $t = 0$ and r is the order of the transformation. A semi-sigmoidal transformation, σ_r, (see [7]) is defined in terms of a sigmoidal transformation by

$$\sigma_r(t) := 2\gamma_r(\frac{t}{2}) = \gamma_r(\frac{t}{2})/\gamma_r(\frac{1}{2}), \quad 0 \leq t \leq 1, \tag{3.2}$$

as $\gamma_r(\frac{1}{2}) = \frac{1}{2}$, by (3.1). It can be shown that σ_r is actually a sigmoidal transformation of the interval [0,2] onto itself [7]. It has been shown computationally [7] and via error analysis [8] that semi–sigmoidal transformations more accurately evaluate integrals of the forms (2.1) and (2.2) than do sigmoidal transformations.

Let us generalise the semi–sigmoidal transformation idea to the $(1/\mathrm{m})^{\mathrm{th}}$ sigmoidal transformation, $\gamma_{r,m}$, mapping [0,1] onto itself and defined by

$$\gamma_{r,m}(t) := \frac{\gamma_r(t/m)}{\gamma_r(1/m)}, \quad 0 \leq t \leq 1, \tag{3.3}$$

where $m \in \mathbb{N}$. The sigmoidal transformation is obtained when $m = 1$ and the semi–sigmoidal transformation is obtained when $m = 2$. Since a transformation with $m = 2$ yields more accurate evaluation of weakly singular integrals than when $m = 1$, it is reasonable therefore to ask, what is $\lim_{m\to\infty} \gamma_{r,m}(t)$? Using equations (3.1) and (3.3) it follows that

$$\lim_{m\to\infty} \gamma_{r,m}(t) = \lim_{m\to\infty} \frac{f_r(t/m)}{f_r(t/m) + f_r(1-t/m)} \frac{f_r(1/m) + f_r(1-1/m)}{f_r(1/m)}. \tag{3.4}$$

Fix $t \in [0,1]$. Since $f_r(\xi) = c_r \xi^r$ near $\xi = 0$, for $m \gg 1$ we have from (3.4) that

$$\lim_{m\to\infty} \gamma_{r,m}(t) = \lim_{m\to\infty} \frac{c_r(t/m)^r}{c_r(t/m)^r + f_r(1-t/m)} \frac{c_r(1/m)^r + f_r(1-1/m)}{c_r(1/m)^r} \tag{3.5}$$

$$= t^r \lim_{m\to\infty} \frac{c_r(1/m)^r + f_r(1-1/m)}{c_r(t/m)^r + f_r(1-t/m)} \tag{3.6}$$

$$= t^r \tag{3.7}$$

since, from (3.1), $f_r(1) \neq 0$. Thus the transformation t^r, which maps [0,1] onto itself, although not a sigmoidal transformation, is a limit of the $(1/\mathrm{m})^{\mathrm{th}}$ sigmoidal transformation as $m \to \infty$.

Based upon the above argument, we define the monomial transformation, μ_r, as

$$\mu_r(t) := t^r, \quad 0 \leq t \leq 1, \tag{3.8}$$

where the order of the transformation, r, does not need to be integral.

The monomial transformation also arises from several other existing transformations. Firstly, consider the transformation of Sato *et al.* [5] (with singularity at $t = -1$)

$$\gamma_r^S(t) = -1 + \frac{1}{2^{r-1}}(1+t)^r \tag{3.9}$$

which is a transformation of [-1,1] onto itself. Now transform the interval [-1,1] (with singularity at -1) onto the interval [0,1] (with singularity at zero) using

$$u = \frac{1+t}{2} \tag{3.10}$$

then

$$\frac{\gamma_r^S(t)+1}{2} = u^r = \mu_r(u), \quad 0 \leq u \leq 1. \tag{3.11}$$

Hence, we see that the monomial transformation on [0,1] is equivalent to the transformation of Sato *et al.* over [-1,1] with singularity at $t = -1$. Using the transformation $u = \frac{1-t}{2}$, it can be shown that the monomial transformation is also equivalent to the transformation of Sato *et al.* with singularity at $t = 1$.

Secondly, consider the Monegato–Sloan transformation (see [12]), which is also a mapping of the interval $[-1,1]$ onto itself, defined by

$$s = \beta_r(t) := s_0 + \delta(s_0, r)(t - t_0)^r \tag{3.12}$$

for an arbitrary singular point s_0, $-1 < s_0 < 1$. We restrict r to being an odd integer and $\delta(s_0, r)$ and t_0 are defined by

$$\delta(s_0, r) = 2^{-r} \left((1 + s_0)^{1/r} + (1 - s_0)^{1/r} \right)^r , \tag{3.13}$$

and

$$t_0 = \frac{(1 + s_0)^{1/r} - (1 - s_0)^{1/r}}{(1 + s_0)^{1/r} + (1 - s_0)^{1/r}}, \tag{3.14}$$

respectively. Now if $s_0 = -1$, say, it follows that $t_0 = -1$ and $\delta(-1, r) = 2^{1-r}$ so that

$$s = \beta_r(t) = -1 + 2^{1-r}(t + 1)^r. \tag{3.15}$$

In this case Monegato and Sloan's restriction of r being an odd integer can be removed and one of the transformations of Sato *et al.* [5] is recovered. Hence, from above, it can be seen that β_r is the generalisation of the monomial transformation on [0,1] to the interval $[-1, 1]$. Similar comments apply to the case where $s_0 = 1$.

Finally, the monomial transformation is also recovered from the transformation of Monegato and Scuderi [15]

$$\gamma_{p,q}(t) = \frac{(p + q - 1)!}{(p - 1)!(q - 1)!} \int_0^t u^{p-1}(1 - u)^{q-1}\, du \tag{3.16}$$

with $q = 1$.

In order to apply the monomial transformation for an arbitrary singularity, $s_0 \in (-1, 1)$, firstly, split the integral at s_0 to give

$$g = \int_{-1}^{s_0} \ln \frac{1}{r(s)} \phi(s) J(s) ds + \int_{s_0}^{1} \ln \frac{1}{r(s)} \phi(s) J(s) ds. \tag{3.17}$$

Next, the variable of integration is changed so that both integrals are evaluated over the range [0,1], ensuring that the point s_0 maps to 0 in both cases. That is, for the first integral in equation (3.17), apply the transformation $s = s_0 - (1 + s_0)t$ and in the second integral apply the transformation $s = s_0 + (1 - s_0)t$, to give

$$\begin{aligned} g = (1 + s_0) \int_0^1 \ln \frac{1}{r(s_0 - (1 + s_0)t)} \phi(s_0 - (1 + s_0)t) J(s_0 - (1 + s_0)t) dt \\ + (1 - s_0) \int_0^1 \ln \frac{1}{r(s_0 + (1 - s_0)t)} \phi(s_0 + (1 - s_0)t) J(s_0 + (1 - s_0)t) dt. \end{aligned} \tag{3.18}$$

The advantage of the monomial transformation (equation (3.8)) is that it can be directly compared with the previously defined semi–sigmoidal transformations [7] through the error analysis described in the paper by Johnston and Elliott [8]. Using the notation of that paper, for the integral defined by

$$I_2(g; \alpha) := \int_{-1}^{1} (1 - \eta)^\alpha \ln(1 - \eta) g(\eta) d\eta, \tag{3.19}$$

where g is an arbitrary "well–behaved" function, an asymptotic estimate for the truncation error when evaluating the transformed integral via n–point Gauss–Legendre quadrature is given by

$$\begin{aligned} E_{2,n,r}(g; \alpha) \sim (2n + 1)^{-2r(1+\alpha)} 2^{3+\alpha-2r(1+\alpha)} r g(1) c_r^{1+\alpha} \Gamma(2r(1 + \alpha)) \\ \times \{-\pi r \cos(\pi(r(1 + \alpha) - 1)) + \sin(\pi(r(1 + \alpha) - 1)) \\ \times [2r \ln(2n + 1) + (2r - 1) \ln 2 - \ln c_r - 2r\psi(2r(1 + \alpha))]\} . \end{aligned} \tag{3.20}$$

The quantity in this equation which depends on the transformation itself is c_r, the coefficient of t^r in the sigmoidal transformation of order r near $t = 0$. For the monomial transformation, $c_r = 1$ for all values of r, which, as can be seen from Table 1, is smaller, for a given r, than the corresponding c_r for any of the sigmoidal or semi–sigmoidal transformations given in [14] and [16]. Hence, for the monomial transformation applied to the integral $I_2(g; \alpha)$ the asymptotic

estimate for the error is given by

$$E_{2,n,r}^{mono}(g;\alpha) \sim (2n+1)^{-2r(1+\alpha)} 2^{3+\alpha-2r(1+\alpha)} r g(1) \Gamma(2r(1+\alpha)) \\ \times \{-\pi r \cos(\pi(r(1+\alpha)-1)) + \sin(\pi(r(1+\alpha)-1)) \\ \times [2r\ln(2n+1) + (2r-1)\ln 2 - 2r\psi(2r(1+\alpha))]\}. \tag{3.21}$$

4 Numerical Examples

In order to assess the utility of the transformation described above and to establish its optimum behaviour, several integrals of importance in the boundary element method are evaluated.

The results are compared in terms of the relative error, defined by

$$\text{relative error} = \left| \frac{I_{approximate} - I_{exact}}{I_{exact}} \right| \tag{4.1}$$

where $I_{approximate}$ and I_{exact} are the approximate and exact values of the integral being considered.

4.1 A Simple Example

Firstly, consider the integral

$$I(s_0) = \int_{-1}^{1} \ln|s - s_0| ds \tag{4.2}$$

which, in terms of the boundary element method, contains the logarithmic kernel and a constant basis function, $\phi(s) \equiv 1$, (the Jacobian, $J(s)$, of the transformation from an arbitrary integral to the one above has been ignored). The integral $I(s_0)$ can be evaluated explicitly as

$$I(s_0) = (\ln(1-s_0) - 1)(1-s_0) + (\ln(1+s_0) - 1)(1+s_0) \tag{4.3}$$

for $-1 < s_0 < 1$ and $I(\pm 1) = 2(\ln 2 - 1)$. This integral has been considered previously as a test integral for other proposed integration schemes for several values of s_0: $s_0 = 1$, $s_0 = -0.3$ [2, 6, 7]; $s_0 = 0.8$ [3, 6, 7].

Now consider evaluating the integral $I(s_0)$ using the monomial transformation, equation (3.8). Recall that to evaluate this integral, the interval of integration must be split at the singularity and each subinterval mapped onto $[0,1]$, with the singularity mapping to 0 in both cases. Hence for a fair comparison, evaluation of the integral $I(s_0)$ using the monomial transformation should use half the number of Gaussian points in each integration that the Telles and Monegato–Sloan transformations can use (that is, there is the same total number of function evaluations in both cases). Figure 1 shows a comparison of truncation errors (the numerator of the relative error (4.1)) between the Telles transformation ($r = 3$ in equation (3.12)), the Monegato–Sloan transformation of orders 5 and 7 (all with 20 Gaussian points) and the monomial transformation of orders 3, 5 and 7 using 10 Gaussian points in each interval.

It can be seen from Figure 1 that even a monomial transformation of order 3 is approximately two orders of magnitude more accurate than the original Telles approach. The figure also shows that, for most values of s_0, the monomial transformation is more accurate than the transformation of Monegato and Sloan, for a given order. The exception to this is when $s_0 = 1$, where 10 points should be used for the Monegato–Sloan transformation which will yield identical results to the monomial transformation. In fact, the truncation error is independent of s_0, a result which can be demonstrated for the integral $I(s_0)$ using the error estimates given by Johnston and Elliott [8]. It turns out that the asymptotic error for the numerical approximation to $I(s_0)$, for integer r, is given by (equation (3.21) with $\alpha = 0$ and $g(1) = 1$)

$$E_{2,n,r}^{mono}(1;0) \sim \frac{(-1)^r 2^{3-2r} r^2 \Gamma(2r)\pi}{(2n+1)^{2r}}, \tag{4.4}$$

independent of s_0.

Increasing the order of the transformation reduces the asymptotic error up to a certain point, then it increases again. An optimal value is predicted numerically at $r = 15$. On the other hand, differentiating the error estimate (4.4) with respect to r, and equating to zero,

gives $r \sim (2n+1)$ as a minimum for $n \gg 1$. Hence for $n = 10$, the minimum error should occur at $r = 21$. The main reason for this discrepancy could be due to lack of working precision on the computer. At $r = 15$, the absolute error is of the order of 10^{-13} (near the working limits of the machine); however, the formula for the error estimate predicts an absolute error of approximately 10^{-15} when $r = 21$. Although these two results are quite close together, it is probably safest to choose the order of the transformation to be equal to the number of Gaussian points used. This may not be optimal, but it tends to err on the side of caution.

4.1.1 Non–Integer Transformation Orders

Interestingly, the error estimate can be improved by using non–integer values for r, the order of the transformation. The asymptotic error for evaluating the integral $I(s_0)$ with a general r is given by

$$E_{2,n,r}^{mono}(1;0) \sim (2n+1)^{-2r} 2^{3-2r} r\Gamma(2r) \times \{-\pi r \cos(\pi(r-1)) + \sin(\pi(r-1)) \left[2r \ln(2n+1) + (2r-1)\ln 2 - 2r\psi(2r)\right]\}. \tag{4.5}$$

Plots of the absolute values of $E_{2,n,r}^{mono}(1;0)$ for $n = 10$ and $n = 20$ are shown in Figures 2 and 3, respectively. The important feature of these curves is the presence of several "inverted" spikes. Each spike corresponds to a value of r at which $E_{2,n,r}^{mono}(1;0)$ is zero (since the graphs are plots of absolute values). These figures also show the actual error for the numerical calculations. It can be seen that the asymptotic error generally agrees very closely with the calculated values. However, for $n = 10$, the asymptotic error underestimates the actual error for orders of transformation greater than about 7. Also, for $n = 20$, round off errors affect the numerical calculation and so it is difficult to make comparisons with the asymptotic errors for orders of transformation greater than about 7.

Based on observations from the above plots, it is theoretically possible to choose a value of r which gives a truncation error of zero, for a given value of n. These values of r can be

obtained as zeros of the transcendental equation

$$\pi r \cot(\pi(r-1)) = 2r \ln(2n+1) + (2r-1)\ln 2 - 2r\psi(2r) \tag{4.6}$$

The first few zeros of this equation for $n = 10$ and $n = 20$ are given in Tables 2 and 3, respectively. These tables also show the values of the calculated truncation and relative errors at these zeros and at the adjacent integer orders of transformation. It can be seen that the zeros of the transcendental equation generally give smaller truncation errors. The exception is when $n = 20$ with transformation orders greater than 7 where round off errors have a considerable effect on the calculated quantities.

4.1.2 Specific Values of s_0

Tables 4, 5 and 6 compare approximate values of the integral $I(s_0)$ obtained from various integration schemes with the exact value, as well as showing the relative error, for the specific values of s_0 at $s_0 = 1$, $s_0 = -0.3$ and $s_0 = 0.8$, respectively. Note that the principal factor in making a fair comparison between methods is the number of function evaluations. Also, in the cases of the the sigmoidal and semi–sigmoidal transformations, the transformation order shown is optimal.

Table 4 shows the results for $s_0 = 1$. Recall that in this situation, since the singularity is at an end point, the Monegato–Sloan and monomial transformations are identical and, further, when these transformations are of order 3, both are identical to the Telles transformation. The table indicates that even at modest transformation orders ($r = 5, 7$) the new transformations provide a more accurate evaluation of the integral $I(1)$ than most of the other methods. The exception is the sixth order (optimal) Sidi transformation which yields more accurate values than the fifth order monomial transformation, but not the sixth order monomial transformation. The values for $I(1)$ determined with the monomial transformation with 10 Gaussian

points are more accurate than the values obtained with the Telles, Sanz–Serna and bicubic transformations, each using 20 Gaussian quadrature points.

The same comments apply to the evaluation of the integral $I(-0.3)$, (Table 5). Generally, the monomial transformations of order five or higher result in the most accurate evaluations, with the sixth order Sidi transformation being the exception. However, a sixth order monomial transformation is more accurate than this Sidi transformation. Note that the monomial transformation of order 3 is equivalent to splitting the interval at the singularity and applying the Telles approach on each subinterval, after mapping these onto $[-1, 1]$.

Finally, the above comments also apply to the results shown in Table 6, for the evaluation of the integral $I(0.8)$.

In each of the above tables non–integer transformation orders for the monomial transformation are also included. These orders are again the zeros of equation 4.6 and are identical for each example as the truncation error is independent of s_0. It can again be seen that having a non–integer transformation order reduces the error in the approximation to the value of the integral and these orders give superior results to the adjacent integer transformation orders.

4.2 Quadratic Basis Functions

Now consider quadratic boundary elements where there are three basis functions: $\phi_1(x) = x(x-1)/2$; $\phi_2(x) = 1 - x^2$ and $\phi_3(x) = x(x+1)/2$. Singular integrals are obtained for each of the node points on the element acting as source points and for each basis function. The five integrals to be evaluated are:

1. basis function $x(x-1)/2$, source point (-1,0) and basis function $x(x+1)/2$, source point (1,0)

$$J_1 = \int_{-1}^{1} \ln(x+1)\frac{x(x-1)}{2}dx = \int_{-1}^{1} \ln(1-x)\frac{x(x+1)}{2}dx = \frac{\ln 64 - 17}{18}$$

2. basis function $x(x-1)/2$, source point (0,0) and basis function $x(x+1)/2$, source point (0,0)

$$J_2 = \int_{-1}^{1} \ln|x| \frac{x(x-1)}{2} dx = \int_{-1}^{1} \ln|x| \frac{x(x+1)}{2} dx = -\frac{1}{9}$$

3. basis function $x(x-1)/2$, source point (1,0) and basis function $x(x+1)/2$, source point (-1,0)

$$J_3 = \int_{-1}^{1} \ln(1-x) \frac{x(x-1)}{2} dx = \int_{-1}^{1} \ln(1+x) \frac{x(x+1)}{2} dx = \frac{\ln 64 + 1}{18}$$

4. basis function $1-x^2$, source point (-1,0) and basis function $1-x^2$, source point (1,0)

$$J_4 = \int_{-1}^{1} \ln(x+1)(1-x^2) dx = \int_{-1}^{1} \ln(1-x)(1-x^2) dx = \frac{2\ln 64 - 10}{9}$$

5. basis function $1-x^2$, source point (0,0)

$$J_5 = \int_{-1}^{1} \ln|x|(1-x^2) dx = -\frac{16}{9}$$

As a final example, consider evaluating the J integrals with the monomial transformation (Table 7). Here, the integrals J_2 and J_5 must be split to apply the transformation and so it should be remembered that twice as many function evaluations are required. Generally, the monomial transformation produces the lowest relative error of all the methods considered. However, there is again the problem of an optimal order. It appears, as in the case of the Monegato–Sloan transformation [11], that the order of the transformation should be numerically equal to half the number of Gaussian points used which is different from the case with the evaluation of the integral $I(s_0)$ using the monomial transformation where the order should be equal to the number of Gaussian points used.

It is also possible to use non–integer transformation orders for the monomial method when evaluating the above integrals. However, an exhaustive study for these integrals would occupy too much space as each integral requires the solution of a slightly different transcendental

to obtain the appropriate transformation orders. However, to illustrate this idea, consider evaluating the integral J_1 with 10 Gaussian points. Using a transformation order of 5.2777 gives a relative error of 3.88×10^{-13} which is much smaller than many other error values obtained. As another example, using a transformation order of 5.1962 when evaluating J_3 with 10 Gaussian points gives a relative error of 1.94×10^{-16}, again much better than most other techniques.

5 Hadamard Finite–Part Integrals

Hadamard finite–part integrals also play a role in the boundary element method. Here it will be shown that the above monomial transformation can also be applied to these integrals.

Consider the integral

$$H(f;s_0,\alpha) = \fint_{-1}^{1} \frac{\operatorname{sgn}(s-s_0)}{|s-s_0|^{1+\alpha}} f(s)\,ds \tag{5.1}$$

where $-1 < s_0 < 1$, $0 < \alpha < 1$, f is a Lipschitz continuous function on $[-1,1]$ and the double bars denote the Hadamard finite–part integral. The integral $H(f;s_0,\alpha)$ can be split at the singularity and rewritten as

$$H(f;s_0,\alpha) = -\fint_{-1}^{s_0} \frac{f(s)}{(s_0-s)^{1+\alpha}}\,ds + \fint_{s_0}^{1} \frac{f(s)}{(s-s_0)^{1+\alpha}}\,ds. \tag{5.2}$$

From [17] we define

$$\fint_a^b \frac{f(t)}{(b-t)^{1+\alpha}}\,dt := \int_a^b \frac{f(t)-f(b)}{(b-t)^{1+\alpha}}\,dt - \frac{f(b)}{\alpha(b-a)^{\alpha}}, \tag{5.3}$$

and

$$\fint_a^b \frac{f(t)}{(t-a)^{1+\alpha}}\,dt := \int_a^b \frac{f(t)-f(a)}{(t-a)^{1+\alpha}}\,dt - \frac{f(a)}{\alpha(b-a)^{\alpha}}. \tag{5.4}$$

Using these definitions, the integral $H(f;s_0,\alpha)$ can again be rewritten as

$$\begin{aligned} H(f;s_0,\alpha) = &-\left\{\int_{-1}^{s_0} \frac{f(s)-f(s_0)}{(s_0-s)^{1+\alpha}}\,ds - \frac{f(s_0)}{\alpha(s_0+1)^{\alpha}}\right\} \\ &+\left\{\int_{s_0}^{1} \frac{f(s)-f(s_0)}{(s-s_0)^{1+\alpha}}\,ds - \frac{f(s_0)}{\alpha(1-s_0)^{\alpha}}\right\} \end{aligned} \tag{5.5}$$

or

$$H(f;s_0,\alpha) = \int_{-1}^{s_0} \frac{f(s_0)-f(s)}{(s_0-s)^{1+\alpha}}\,ds + \int_{s_0}^{1} \frac{f(s)-f(s_0)}{(s-s_0)^{1+\alpha}}\,ds + \frac{f(s_0)}{\alpha(s_0+1)^{\alpha}} - \frac{f(s_0)}{\alpha(1-s_0)^{\alpha}}. \tag{5.6}$$

The two integrals in equation (5.6) are now weakly singular and so can be evaluated using the monomial transformation. Hence, in order to obtain a value for the Hadamard finite–part integral, $H(f;s_0,\alpha)$, we proceed as follows:

1. Map both integrals in equation (5.6) onto the interval [0,1] with s_0 mapping to 0 (c.f. equations (3.17) and (3.18)),

2. Apply the transformation $\mu_r(s) = s^r$ to both integrals,

3. Evaluate the integrals using Gaussian Quadrature,

4. Add the additional terms in equation (5.6).

As an example to illustrate this method, consider the following integral

$$H(e^s;0.2,0.2) = \oint_{-1}^{1} \frac{\mathrm{sgn}(s-0.2)}{|s-0.2|^{1.2}} e^s\,ds. \tag{5.7}$$

The integral has previously been considered by Kutt [18] and is also used as an illustrative example for the bicubic transformation method of Cerrolaza and Alarcon [3]. The value for the integral given by Kutt is 2.4464143506. Using 14 Gaussian quadrature points on each subinterval (28 function evaluations) the bicubic transformation yields a value for the integral of 2.4463. Application of the method outlined above to this integral yields a value of 2.4464170777 using only six Gaussian points (12 function evaluations) and a fourth order monomial transformation. This value can be improved to give 2.4464143408 by using 14 Gaussian points (28 function evaluations) and a fifth order transformation. By firstly splitting the interval of integration at the singularity and then integrating by parts twice, *Mathematica* yields a value of

$H(e^s; 0.2, 0.2) = 2.446414340789413$. The results for the evaluation of this integral are shown in Table 8.

It is possible to extend the above approach to a more general exponent α in the denominator of equation (5.1). Let α be such that $n < \alpha < n+1$ where $n \in \{0, 1, 2, \ldots\}$, then, following Elliott [17], take a Taylor series of the function f about the point s_0. This is given by

$$f(s) = f_n(s) + \frac{1}{\Gamma(n+1)} \int_{s_0}^{s} f^{(n+1)}(y)(s-y)^n \, dy \tag{5.8}$$

where

$$f_n(s) = \sum_{k=0}^{n} \frac{f^{(k)}(s_0)(s-s_0)^k}{\Gamma(k+1)}. \tag{5.9}$$

Then, following some algebra, it can be shown that

$$\begin{aligned} H(f; s_0, \alpha) = & \int_{-1}^{s_0} \frac{f_n(s) - f(s)}{(s_0 - s)^{1+\alpha}} \, ds + \int_{s_0}^{1} \frac{f(s) - f_n(s)}{(s - s_0)^{1+\alpha}} \, ds \\ & - \sum_{k=0}^{n} \frac{f^{(k)}(s_0)}{(\alpha - k)\Gamma(k+1)} \left[\frac{(-1)^{(k+1)}}{(s_0+1)^{\alpha-k}} + \frac{1}{(1-s_0)^{\alpha-k}} \right]. \end{aligned} \tag{5.10}$$

The two integrals in this expression are again weakly singular and so can be evaluated as suggested above.

The above concept also applies to integer values of α. Here, the resulting integrals in equation (5.10) are regular and so standard Gauss–Legendre quadrature can be applied in their evaluation. This is, of course, equivalent to a monomial transformation of order 1. In particular, $\alpha = 0$ corresponds to a Cauchy principal value integral and equation (5.10) would correspond to the so–called 'bootstrap' techniques, applied to the boundary element method by Guiggiani and Casalini [19].

6 Conclusion

This paper has introduced a monomial transformation with Gaussian quadrature to improve the accuracy of evaluating both weakly and strongly singular integrals. The transformation

arises from several other previously published transformations with the underlying idea being to utilise the same Gaussian quadrature points used for evaluating non–singular integrals in a typical boundary element method implementation. The method requires the original interval to be split at the singularity and the two subintervals mapped onto $[0, 1]$ with the singularity mapped to 0 in both cases. Although the method requires some degree of pre–implementation algebra, it generally yields more accurate numerical results for the same number of function evaluations than existing transformations. The transformation has also been shown to be equivalent to other existing transformations in certain cases.

The technique has been implemented and numerically compared with other coordinate transformations and interval splitting techniques for two different types of integrals applicable in a boundary element method context. Generally, the new techniques are numerically superior to the existing methods, with, as mentioned above, the monomial transformation performing better than the recently introduced Monegato–Sloan transformation [12, 13, 11]. The technique has also been shown to be able to evaluate accurately certain Hadamard finite–part integrals.

The only question which arises with these new methods is: what order of transformation is optimal? Utilising too higher an order of transformation tends to increase the relative error. For the integrals $I(s_0)$, generally choosing the order numerically equal to the number of Gaussian points seems appropriate, yet for the J integrals, an order equal to half the number of Gaussian points is indicated. The asymptotic error estimates show that it is possible to improve the accuracy of the numerical calculations by using non–integer orders of transformation.

In summary, the monomial transformation presented above, with an order equal to half the number of Gaussian points used, generally yields more accurate values for the integrals described above than the other methods presented. Alternatively, non–integer orders of transformation obtained by solving equation (4.6) can also yield accurate evaluations of the weakly singular integrals.

References

[1] J. H. Kane, *Boundary Element Analysis in Engineering Continuum Mechanics.* Prentice Hall, 1994.

[2] J. C. F. Telles, "A self–adaptive co–ordinate transformation for efficient numerical evaluation of general boundary element integrals," *International Journal for Numerical Methods in Engineering*, vol. 24, pp. 959–973, 1987.

[3] M. Cerrolaza and E. Alarcón, "A bi–cubic transformation for the numerical evaluation of the Cauchy principal value integrals in boundary methods," *International Journal for Numerical Methods in Engineering*, vol. 28, pp. 987–999, 1989.

[4] J. Sanz-Serna, M. Doblaré, and E. Alarcón, "Remarks on methods for the computation of boundary-element integrals by co-ordinate transformation," *Communications in Numerical Methods in Engineering.*, vol. 6, pp. 121–123, 1990.

[5] M. Sato, S. Yoshioka, and K. Tsukui, "Accurate numerical integration of singular kernels in the two–dimensional boundary element method," in *Boundary Elements X, Vol 1* (C. A. Brebbia, ed.), pp. 279–298, Springer–Verlag, 1988.

[6] P. R. Johnston, "Application of sigmoidal transformations to weakly singular and near singular boundary element integrals," *International Journal for Numerical Methods in Engineering*, vol. 45, pp. 1333–1348, August 1999.

[7] P. R. Johnston, "Semi–sigmoidal transformations for evaluating weakly singular boundary element integrals," *International Journal for Numerical Methods in Engineering*, vol. 47, no. 10, pp. 1709–1730, 2000.

[8] P. R. Johnston and D. Elliott, "Error estimation of quadrature rules for evaluating singular integrals in boundary element problems," *International Journal for Numerical Methods in Engineering.*, vol. 48, no. 7, pp. 949–962, 2000.

[9] A. H. Stroud and D. Secrest, *Gaussian Quadrature Formulas.* Englewood Cliffs, N.J.: Prentice–Hall, 1966.

[10] G. Beer and J. O. Watson, *Introduction to Finite and Boundary Element Methods for Engineers.* Chichester, England: Wiley, 1992.

[11] P. R. Johnston and D. Elliott, "A generalisation of Telles' method for evaluating weakly singular boundary element integrals," *Journal of Computational and Applied Mathematics*, vol. 131, pp. 223–241, June 2001.

[12] G. Monegato and I. H. Sloan, "Numerical solution of the generalised airfoil equation for an airfoil with a flap," *SIAM Journal of Numerical Analysis*, vol. 34, no. 6, pp. 2288–2305, 1997.

[13] L. Scuderi, "A collocation method for the generalised airfoil equation for an airfoil with a flap," *SIAM Journal of Numerical Analysis*, vol. 35, no. 5, pp. 1725–1739, 1998.

[14] D. Elliott, "Sigmoidal transformations and the trapezoidal rule," *Journal of the Australian Mathematical Society Series B (E)*, vol. 40, pp. E77–E137, 1998.

[15] G. Monegato and L. Scuderi, "High order methods for weakly singular integral equations with non smooth input functions," *Math. Comput.*, vol. 67, pp. 1493–1515, 1998.

[16] A. Sidi, "A new variable transformation for numerical integration," in *Numerical Integration IV* (H. Brass and G. Hammerlin, eds.), pp. 359–373, Birkhauser–Verlag, 1993.

[17] D. Elliott, "An asymptotic analysis of two algorithms for certain Hadamard finite-part integrals," *IMA Journal of Numerical Analysis*, vol. 13, pp. 445–462, 1993.

[18] H. R. Kutt, "Quadrature formulas for finite-part integrals," Tech. Rep. Report Wisk 178, The National Institute for Mathematical Sciences, Pretoria, 1975.

[19] M. Giuggiani and P. Casalini, "Direct computation of Cauchy principal value integrals in advanced boundary elements," *International Journal for Numerical Methods in Engineering*, vol. 24, pp. 1711–1720, 1987.

Captions

Table 1: Values of the coefficient c_r for various orders of sigmoidal and semi–sigmoidal Sidi and Elliott transformations.

Table 2: Truncation and relative errors for the integral $I(1)$ obtained using the monomial method for various orders of transformation and 10 Gaussian points. The non–integer transformation orders are the zeros of equation (4.6) with $n = 10$.

Table 3: Truncation and relative errors for the integral $I(1)$ obtained using the monomial method for various orders of transformation and 20 Gaussian points. The non–integer transformation orders are the zeros of equation (4.6) with $n = 20$.

Table 4: Approximate values and relative errors for the integral $I(1)$, obtained using the various integration schemes with various numbers of Gaussian integration points and (where appropriate) various orders of transformation. The number of function evaluations for each integration scheme at the given number of Gaussian integration points is also shown. The non–integer transformation orders for the monomial transformation are the zeros of equation (4.6) with $n = 10$.

Table 5: Approximate values and relative errors for the integral $I(-0.3)$, obtained using the various integration schemes with various numbers of Gaussian integration points and (where appropriate) various orders of transformation. The number of function evaluations for each integration scheme at the given number of Gaussian integration points is also shown. The non–integer transformation orders for the monomial transformation are the zeros of equation (4.6) with $n = 10$.

Table 6: Approximate values and relative errors for the integral $I(0.8)$, obtained using the various integration schemes with various numbers of Gaussian integration points and (where appropriate) various orders of transformation. The number of function evaluations for each

integration scheme at the given number of Gaussian integration points is also shown. The non–integer transformation orders for the monomial transformation are the zeros of equation (4.6) with $n = 10$.

Table 7: Relative errors for the integrals J_1, J_2, J_3, J_4 and J_5 comparing the monomial transformation to other previously published transformations. Here the integrals J_2 and J_5 contain an interior singularity, hence the number of function evaluations is twice the number of Gaussian quadrature points for the bicubic and monomial transformation methods and equal to the number of Gaussian quadrature points for the other methods, as well as for the remaining integrals.

Table 8: Values of the integral $H(e^s; 0.2, 0.2)$ obtained using the bicubic transformation [3] and equation (5.6) using various numbers of Gaussian integration points and orders of transformation.

Figure 1: Plot of the absolute value of the truncation error for evaluation of the integral $I(s_0)$ as the singularity offset, s_0, varies from 0 to 1. Integration is performed with the Telles method and the Monegato–Sloan transformation of orders 5 and 7 utilising 20 Gaussian quadrature points and the monomial transformation of orders 3, 5 and 7, utilising 10 Gaussian quadrature points, yet requiring 20 function evaluations.

Figure 2: Plot of the absolute value of the truncation error obtained from equation (4.5) with $n = 10$ (dotted line) and from computations (solid line) using 10 Gaussian points. The grid lines emphasise the position of the integer transformation orders.

Figure 3: Plot of the absolute value of the truncation error obtained from equation (4.5) with $n = 20$ (dotted line) and from computations (solid line) using 20 Gaussian points.

Transformation	Sidi Transformation [16]		Elliott Transformation [14]	
Order (r)	Sigmoidal	Semi–Sigmoidal	Sigmoidal	Semi–Sigmoidal
2	$\frac{\pi^2}{4}$	$\frac{\pi^2}{8}$	—	—
3	$\frac{2\pi^2}{3}$	$\frac{\pi^2}{6}$	$\frac{2\pi^2}{3}$	$\frac{\pi^2}{6}$
4	$\frac{3\pi^4}{16}$	$\frac{3\pi^4}{128}$	—	—
5	$\frac{8\pi^4}{15}$	$\frac{\pi^4}{30}$	$\frac{6\pi^4}{5}$	$\frac{3\pi^4}{40}$
6	$\frac{5\pi^6}{32}$	$\frac{5\pi^6}{1024}$	—	—
7	$\frac{16\pi^6}{35}$	$\frac{\pi^6}{140}$	$\frac{20\pi^6}{7}$	$\frac{5\pi^6}{112}$

Table 1:

Transformation Order	|Truncation Error|	Relative Error
1	1.15×10^{-2}	1.87×10^{-2}
1.16144	4.09×10^{-5}	6.67×10^{-5}
2	1.67×10^{-4}	2.72×10^{-4}
2.19614	1.12×10^{-6}	1.82×10^{-6}
3	4.58×10^{-6}	7.47×10^{-6}
3.22443	3.03×10^{-8}	4.93×10^{-8}
4	2.08×10^{-7}	3.38×10^{-7}
4.24946	1.65×10^{-9}	2.70×10^{-9}
5	1.43×10^{-8}	2.33×10^{-8}
5.27234	1.59×10^{-10}	2.59×10^{-10}
6	1.41×10^{-9}	2.30×10^{-9}
6.29361	2.27×10^{-11}	3.70×10^{-11}
7	1.92×10^{-10}	3.13×10^{-10}
7.31357	4.47×10^{-12}	7.28×10^{-12}
8	3.52×10^{-11}	5.73×10^{-11}
8.33240	1.16×10^{-12}	1.89×10^{-12}
9	8.43×10^{-12}	1.37×10^{-11}
9.35021	3.86×10^{-13}	6.29×10^{-13}
10	2.62×10^{-12}	4.27×10^{-12}

Table 2:

Transformation Order	|Truncation Error|	Relative Error
1	3.01×10^{-3}	4.90×10^{-3}
1.13364	6.97×10^{-6}	1.14×10^{-5}
2	1.14×10^{-5}	1.86×10^{-5}
2.15782	5.05×10^{-8}	8.24×10^{-8}
3	8.09×10^{-8}	1.32×10^{-7}
3.17690	2.64×10^{-10}	4.31×10^{-10}
4	9.35×10^{-10}	1.52×10^{-9}
4.19346	2.53×10^{-12}	4.12×10^{-12}
5	1.62×10^{-11}	2.64×10^{-11}
5.20845	4.70×10^{-14}	7.65×10^{-14}
6	3.91×10^{-13}	6.38×10^{-13}
6.22235	7.77×10^{-16}	1.27×10^{-15}
7	1.51×10^{-14}	2.46×10^{-14}
7.23543	2.22×10^{-15}	3.62×10^{-15}
8	1.67×10^{-15}	2.71×10^{-15}
8.24784	2.33×10^{-15}	3.80×10^{-15}
9	2.22×10^{-15}	3.62×10^{-15}
9.25953	2.33×10^{-15}	3.80×10^{-15}
10	2.11×10^{-15}	3.44×10^{-15}

Table 3:

Integration Method	Nodes	Function Evaluations	Order	Quadrature Approximation	Relative Error
Telles[2]	10	10	—	-0.613701054	7.47×10^{-6}
	20	20	—	-0.613705558	1.32×10^{-7}
Sanz–Serna[4]	10	10	—	-0.636944787	3.78×10^{-2}
	20	20	—	-0.618233902	7.37×10^{-3}
Bicubic[3]	10	10	—	-0.614206553	8.16×10^{-4}
	20	20	—	-0.614199611	8.05×10^{-4}
Sigmoidal Transformations [6]					
Simple	10	10	2	-0.613870561	2.69×10^{-4}
Sidi	10	10	6	-0.613704893	1.21×10^{-6}
Elliott	10	10	3	-0.613675583	4.90×10^{-5}
Semi–Sigmoidal Transformations[7]					
Simple	10	10	4	-0.613704922	1.16×10^{-6}
Sidi	10	10	6	-0.613705645	1.05×10^{-8}
Elliott	10	10	7	-0.613705559	1.30×10^{-7}
Monegato–Sloan Transformations [12]					
	10	10	5	-0.613705625	2.32×10^{-8}
	10	10	7	-0.613705639	3.13×10^{-10}
Monomial Transformations					
	10	10	5	-0.613705625	2.32×10^{-8}
	10	10	5.27234	-0.613705639	2.59×10^{-10}
	10	10	6	-0.613705640	2.30×10^{-9}
	10	10	6.29361	-0.613705639	3.70×10^{-11}
	10	10	7	-0.613705639	3.13×10^{-10}
	10	10	7.31357	-0.613705639	7.28×10^{-12}
	10	10	8	-0.613705639	5.73×10^{-11}
	10	10	8.33240	-0.613705639	1.89×10^{-12}
	10	10	9	-0.613705639	1.37×10^{-11}
	10	10	9.35021	-0.613705639	6.29×10^{-13}
	10	10	10	-0.613705639	4.27×10^{-12}
Exact	—	—	—	-0.613705639	—

Table 4:

Integration Method	Nodes	Function Evaluations	Order	Quadrature Approximation	Relative Error
Telles[2]	10	10	—	-1.903280847	2.78×10^{-3}
	20	20	—	-1.908001667	3.13×10^{-4}
	30	30	—	-1.909028486	2.25×10^{-4}
Sanz–Serna[4]	10	10	—	-1.919845628	5.89×10^{-3}
	20	20	—	-1.910086538	7.79×10^{-4}
	30	30	—	-1.909049250	2.36×10^{-4}
Bicubic[3]	8	16	—	-1.909620476	5.35×10^{-4}
	10	20	—	-1.909606313	5.28×10^{-4}
	12	24	—	-1.909597834	5.23×10^{-4}
Sigmoidal Transformations [6]					
Simple	10	20	2	-1.908762751	8.58×10^{-5}
Sidi	10	20	6	-1.908598116	4.20×10^{-7}
Elliott	10	20	3	-1.908568861	1.57×10^{-5}
Semi–Sigmoidal Transformations[7]					
Simple	10	20	4	-1.908598452	2.44×10^{-7}
Sidi	10	20	6	-1.908598923	3.37×10^{-9}
Elliott	10	20	7	-1.908598837	4.18×10^{-8}
Monegato–Sloan Transformations [12]					
	20	20	5	-1.908624812	1.36×10^{-5}
	20	20	7	-1.908598686	3.37×10^{-7}
	20	20	9	-1.908598904	6.88×10^{-9}
Monomial Transformations					
	10	20	3	-1.908594332	2.40×10^{-6}
	10	20	3.22443	-1.908598978	3.19×10^{-8}
	10	20	4	-1.908599124	1.08×10^{-7}
	10	20	4.24946	-1.908598915	9.74×10^{-10}
	10	20	5	-1.908598903	7.48×10^{-9}
	10	20	5.27234	-1.908598917	3.05×10^{-11}
	10	20	6	-1.908598918	7.39×10^{-10}
	10	20	6.29361	-1.908598917	1.50×10^{-12}
	10	20	7	-1.908598917	1.01×10^{-10}
	10	20	7.31357	-1.908598917	9.93×10^{-13}
	10	20	8	-1.908598917	1.84×10^{-11}
	10	20	8.33240	-1.908598917	3.68×10^{-13}
	10	20	9	-1.908598917	4.42×10^{-12}
	10	20	9.35021	-1.908598917	1.47×10^{-13}
	10	20	10	-1.908598917	1.37×10^{-12}
Exact	—	—	—	-1.908598917	—

Table 5:

Integration Method	Nodes	Function Evaluations	Order	Quadrature Approximation	Relative Error
Telles[2]	10	10	—	-1.267467471	2.84×10^{-3}
	20	20	—	-1.263490728	3.01×10^{-4}
	30	30	—	-1.263522749	2.76×10^{-4}
Sanz–Serna[4]	10	10	—	-1.275118510	8.89×10^{-3}
	20	20	—	-1.265359207	1.17×10^{-3}
	30	30	—	-1.264321919	3.56×10^{-4}
Bicubic[3]	8	16	—	-1.2646	5.76×10^{-4}
	10	20	—	-1.2637	1.36×10^{-4}
	12	24	—	-1.2638	5.66×10^{-5}
Sigmoidal Transformations [6]					
Simple	10	20	2	-1.264035961	1.30×10^{-4}
Sidi	10	20	6	-1.263870813	6.12×10^{-7}
Elliott	10	20	3	-1.263841530	2.37×10^{-5}
Semi–Sigmoidal Transformations [7]					
Simple	10	20	4	-1.263870995	4.67×10^{-7}
Sidi	10	20	6	-1.263871592	5.09×10^{-9}
Elliott	10	20	7	-1.263871506	6.31×10^{-8}
Monegato–Sloan Transformations [12]					
	20	20	5	-1.263888702	1.35×10^{-5}
	20	20	7	-1.263872297	5.63×10^{-7}
	20	20	9	-1.263871580	4.80×10^{-9}
Monomial Transformations					
	10	20	3	-1.263867001	3.63×10^{-6}
	10	20	3.22443	-1.263871601	1.22×10^{-8}
	10	20	4	-1.263871793	1.64×10^{-7}
	10	20	4.24946	-1.263871586	8.65×10^{-11}
	10	20	5	-1.263871571	1.13×10^{-8}
	10	20	5.27234	-1.263871586	3.94×10^{-11}
	10	20	6	-1.263871587	1.12×10^{-9}
	10	20	6.29361	-1.263871586	1.01×10^{-11}
	10	20	7	-1.263871585	1.52×10^{-10}
	10	20	7.31357	-1.263871586	2.51×10^{-12}
	10	20	8	-1.263871586	2.78×10^{-11}
	10	20	8.33240	-1.263871586	7.36×10^{-13}
	10	20	9	-1.263871586	6.67×10^{-12}
	10	20	9.35021	-1.263871586	2.63×10^{-13}
	10	20	10	-1.263871586	2.07×10^{-12}
Exact	—	—	—	-1.263871586	—

Table 6:

Integration Method	Nodes	Order (r)	J_1	J_2	J_3	J_4	J_5
Telles[2]	10		6.43×10^{-6}	1.91×10^{-5}	1.24×10^{-9}	7.57×10^{-9}	6.33×10^{-3}
	20		1.13×10^{-7}	3.45×10^{-8}	3.39×10^{-13}	2.11×10^{-12}	8.37×10^{-4}
	30		1.04×10^{-8}	9.15×10^{-10}	3.87×10^{-16}	1.89×10^{-14}	2.53×10^{-4}
Sanz–Serna[4]	10		3.22×10^{-2}	1.90×10^{-5}	2.87×10^{-4}	1.78×10^{-3}	6.32×10^{-3}
	20		6.33×10^{-3}	3.44×10^{-8}	1.13×10^{-5}	6.98×10^{-5}	8.36×10^{-4}
	30		2.54×10^{-3}	9.14×10^{-10}	2.12×10^{-6}	1.30×10^{-5}	2.53×10^{-4}
Bicubic[3]	6		6.31×10^{-4}	1.80×10^{-7}	1.04×10^{-6}	6.41×10^{-6}	5.63×10^{-4}
	8		7.00×10^{-4}	2.38×10^{-7}	1.67×10^{-6}	1.03×10^{-5}	5.74×10^{-4}
	10		7.00×10^{-4}	2.13×10^{-7}	1.67×10^{-6}	1.03×10^{-5}	5.66×10^{-4}
Monegato and Sloan [12] $\beta_r(t)$	10	3	6.43×10^{-6}	1.91×10^{-5}	1.24×10^{-9}	7.57×10^{-9}	6.33×10^{-3}
		5	2.00×10^{-8}	6.06×10^{-6}	2.52×10^{-12}	1.47×10^{-11}	5.46×10^{-4}
		7	8.77×10^{-10}	6.97×10^{-4}	2.85×10^{-9}	8.75×10^{-9}	3.87×10^{-6}
		9	2.78×10^{-6}	1.34×10^{-2}	6.92×10^{-6}	2.12×10^{-5}	1.69×10^{-3}
		11	9.10×10^{-5}	5.23×10^{-2}	2.27×10^{-4}	6.95×10^{-4}	6.53×10^{-3}
	20	3	1.13×10^{-7}	3.45×10^{-8}	3.39×10^{-13}	2.11×10^{-12}	8.37×10^{-4}
		5	2.27×10^{-11}	6.03×10^{-11}	4.65×10^{-15}	1.04×10^{-15}	1.82×10^{-5}
		7	2.74×10^{-14}	1.46×10^{-12}	5.04×10^{-15}	5.79×10^{-15}	6.67×10^{-7}
		9	3.11×10^{-16}	3.25×10^{-13}	3.49×10^{-15}	1.01×10^{-14}	3.88×10^{-8}
		11	1.56×10^{-16}	9.48×10^{-13}	2.13×10^{-15}	1.11×10^{-14}	3.35×10^{-9}
	30	3	1.04×10^{-8}	9.15×10^{-10}	3.87×10^{-16}	1.89×10^{-14}	2.53×10^{-4}
		5	4.20×10^{-13}	1.21×10^{-13}	3.49×10^{-15}	5.94×10^{-15}	2.46×10^{-6}
		7	7.78×10^{-16}	2.75×10^{-15}	4.26×10^{-15}	6.53×10^{-15}	4.03×10^{-8}
		9	6.23×10^{-16}	5.50×10^{-15}	5.04×10^{-15}	2.23×10^{-15}	1.03×10^{-9}
		11	3.11×10^{-16}	7.24×10^{-15}	5.04×10^{-15}	2.67×10^{-15}	3.85×10^{-11}
Monomial $\mu_r(t)$	10	3	6.43×10^{-6}	4.22×10^{-12}	1.24×10^{-9}	7.57×10^{-9}	2.58×10^{-6}
		5	2.00×10^{-8}	1.54×10^{-13}	2.52×10^{-12}	1.47×10^{-11}	8.03×10^{-9}
		7	8.77×10^{-10}	1.78×10^{-9}	2.85×10^{-9}	8.75×10^{-9}	3.31×10^{-10}
		9	2.78×10^{-6}	4.08×10^{-6}	6.92×10^{-6}	2.12×10^{-5}	5.10×10^{-7}
		11	9.10×10^{-5}	1.28×10^{-4}	2.27×10^{-4}	6.95×10^{-4}	1.60×10^{-5}
	20	3	1.13×10^{-7}	5.39×10^{-16}	3.39×10^{-13}	2.11×10^{-12}	4.55×10^{-8}
		5	2.27×10^{-11}	8.65×10^{-16}	2.13×10^{-15}	1.04×10^{-15}	9.10×10^{-12}
		7	1.65×10^{-14}	1.75×10^{-15}	9.68×10^{-16}	5.79×10^{-15}	7.12×10^{-15}
		9	9.34×10^{-16}	2.62×10^{-15}	7.75×10^{-16}	1.01×10^{-14}	6.25×10^{-16}
		11	1.56×10^{-16}	3.50×10^{-15}	2.13×10^{-15}	1.11×10^{-14}	2.50×10^{-16}
	30	3	1.04×10^{-8}	9.99×10^{-16}	3.87×10^{-16}	1.89×10^{-14}	4.18×10^{-9}
		5	4.20×10^{-13}	1.87×10^{-15}	5.81×10^{-16}	5.94×10^{-15}	1.68×10^{-13}
		7	6.23×10^{-16}	2.75×10^{-15}	2.32×10^{-15}	6.53×10^{-15}	6.25×10^{-16}
		9	1.56×10^{-16}	2.75×10^{-15}	3.10×10^{-15}	2.23×10^{-15}	6.25×10^{-16}
		11	1.09×10^{-15}	2.75×10^{-15}	3.10×10^{-15}	2.67×10^{-15}	1.12×10^{-15}

Table 7:

Integration Method	Nodes	Order (r)	$H(e^s; 0.2, 0.2)$
Bicubic [3]	6	—	1.8527
	8	—	2.3340
	10	—	2.4161
	12	—	2.4381
	14	—	2.4463
Monomial Transformation ($\mu_r(t)$)	6	1	2.4237967672518645
		2	2.4475356352225854
		3	2.4463411780657549
		4	2.4464170776621725
		5	2.4464042804000257
		6	2.4463837836628519
	8	1	2.4317114729771538
		2	2.4468866061407848
		3	2.4463945358188206
		4	2.4464151732102102
		5	2.4464142831323148
		6	2.4464136505780085
	10	1	2.4359366648979179
		2	2.4466537812436022
		3	2.4464072227470863
		4	2.4464145524817416
		5	2.4464143404615943
		6	2.4464143366994762
	12	1	2.4384903781581060
		2	2.4465511606749515
		3	2.4464112737280366
		4	2.4464144094011337
		5	2.4464143407888552
		6	2.4464143405025225
	14	1	2.4401668485611978
		2	2.4464993422672459
		3	2.4464128411487094
		4	2.4464143671516903
		5	2.4464143407894703
		6	2.4464143407297541

Table 8:

0.01
0.0001
1e-06
1e-08
1e-10
1e-12
1e-14
|Truncation Error|
0
0.2
0.4
0.6
0.8
1
Value of s_0
Original Telles
Order 5 Monegato-Sloan
Order 7 Monegato-Sloan
Order 3 Monomial 10
Order 5 Monomial 10
Order 7 Monomial 10

Figure 1:

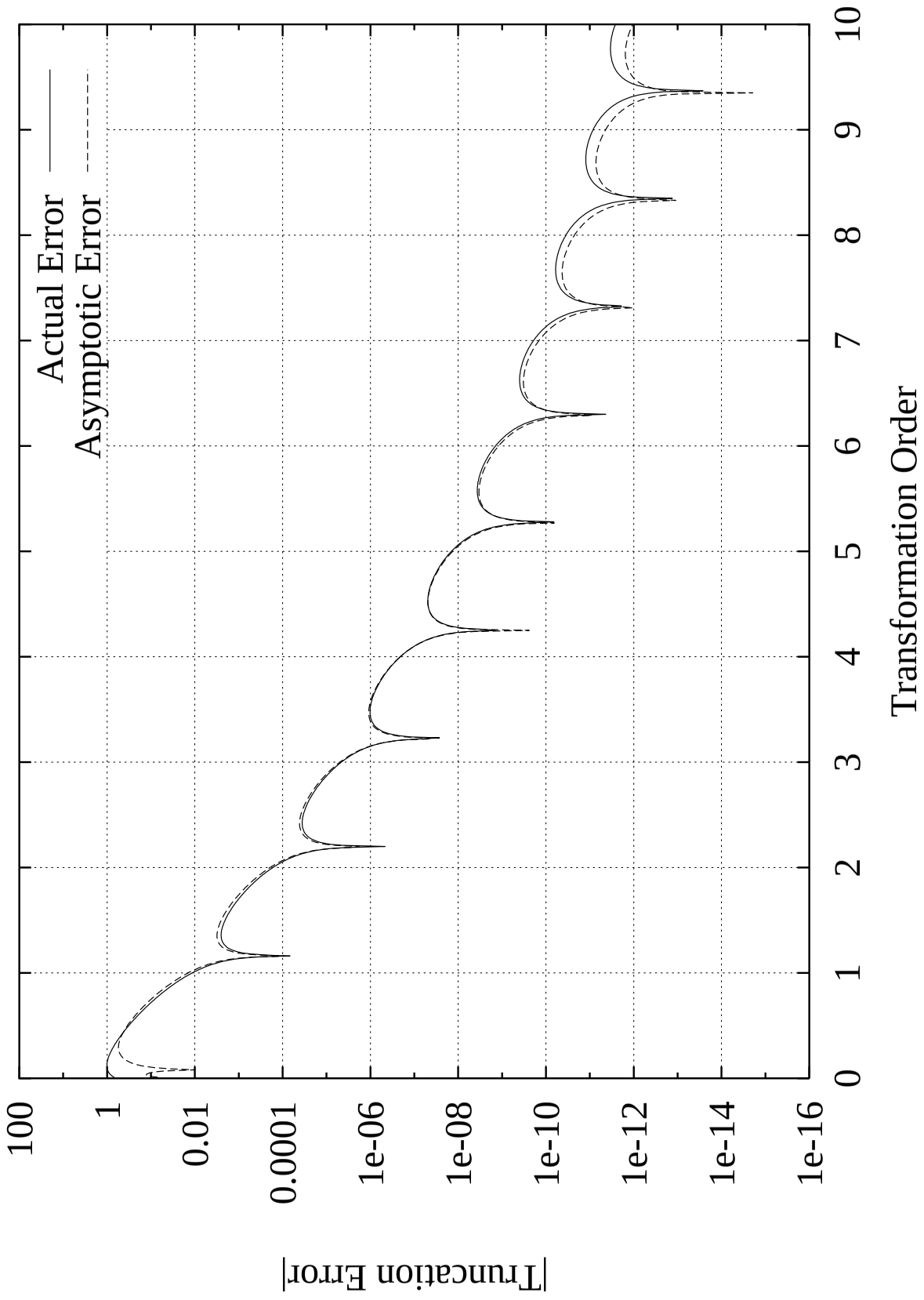
Actual Error
Asymptotic Error
|Truncation Error|
Transformation Order
100
1
0.01
0.0001
1e-06
1e-08
1e-10
1e-12
1e-14
1e-16
0
1
2
3
4
5
6
7
8
9
10

Figure 2:

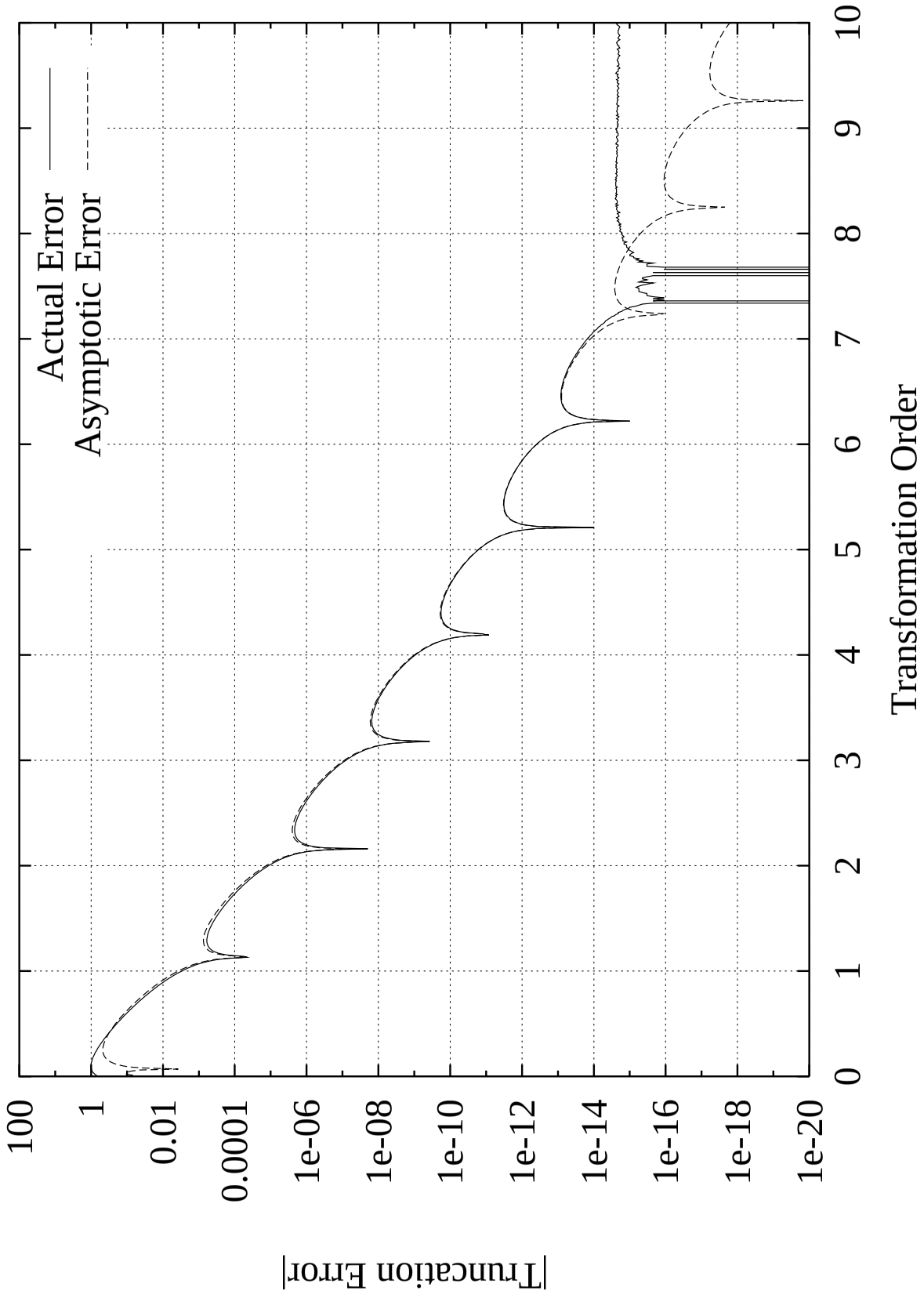
Actual Error
Asymptotic Error
|Truncation Error|
Transformation Order
100
1
0.01
0.0001
1e-06
1e-08
1e-10
1e-12
1e-14
1e-16
1e-18
1e-20
0
1
2
3
4
5
6
7
8
9
10

Figure 3: